Journal of Archaeological Science 41 (2014) 856–867

Contents lists available at ScienceDirect

Journal of Archaeological Science

journal homepage: http://www.elsevier.com/locate/jas

Archaeomagnetic study and dating at five sites from Catalonia (NE Spain)

Lluís Casas [a,*], Marta Prevosti [b], Boutheina Fouzai [c], Aureli Álvarez [a]

[a] Universitat Autònoma de Barcelona, Facultat de Ciències, Departament de Geologia, Campus de la UAB, 08193 Bellaterra, Catalonia, Spain
[b] Institut Català d'Arqueologia Clàssica, Plaça d'en Rovellat, s/n, 43003 Tarragona, Catalonia, Spain
[c] Université de Tunis El Manar, Faculté des Sciences, Département de Géologie, Campus Universitaire, 2092 Manar II, Tunisia

ARTICLE INFO

Article history:
Received 21 August 2013
Received in revised form
14 October 2013
Accepted 17 October 2013

Keywords:
Archaeomagnetism
Pottery
Typology
Dating
Geomagnetic field modeling
Archaeodirection
Archaeointensity

ABSTRACT

Archaeomagnetic dating techniques have been applied to constrain the age of kilns from five archaeological sites in Catalonia (NE Spain). The SCHA.DIF.3K regional archaeomagnetic model and the secular variation curve for the Iberian Peninsula were used. Three sites (Vil·la de Barenys, La Buada and Collet de Sant Antoni) produced typologically datable artifacts and the archaeomagnetic-direction dating of their kilns agrees roughly with the archaeological ages. Two kilns, at Sota la Timba del Castellot (TC) and Riera de la Selva (RS) appeared isolated lacking of datable artefacts and their archaeomagnetic directions bring important information on their age. For example, the result at RS could be an evidence of the survival of kilns of Roman type (Cuomo di Caprio II/c or Le Ny IIF) up to late Antiquity. Archaeointensities were also obtained for two kilns (La Buada and TC), the first is a datum that can be used as a reference point to improve the description of the archaeointensity variation during Roman times and the latter was used to constrain further the age of kiln TC and confirming its Antique age.

1. Introduction

Archaeomagnetism encompasses a number of techniques and methods that retrieve past values of the Earth's magnetic field from archaeological baked materials. Its main goal is to track the evolution of the geomagnetic field and to use it as a dating tool. Archaeomagnetic studies are progressing continuously all around the world and particularly in Europe, where the early developments in archaeomagnetism took place (Wolfman, 1991).

The constant progress of archaeomagnetism promotes that more and better reference secular variation curves (SVC) be available (e.g. Schnepp and Lanos, 2005; Zananiri et al., 2007; Kovacheva et al., 2009) and wider time ranges be covered (Tema and Kondopoulou, 2011; Fanjat et al., 2013; Hervé et al., 2011). Besides SVC, geomagnetic field models are also being developed (e.g. Korte et al., 2009) and regularly updated (e.g. Korte and Constable, 2011).

In 2006, a SVC for the Iberian Peninsula was established (Gómez-Paccard et al., 2006a) and, soon after, Spanish researchers developed a geomagnetic field model (SCHA.DIF.3K) not only for Iberia but the whole European continent and neighboring areas (Pavón-Carrasco et al., 2009). Despite the relatively scarce Iberian archaeomagnetic data corresponding to the Roman period (Gómez-Paccard et al., 2006b; Ruiz-Martínez et al., 2008) both the Iberian SVC and the SCHA.DIF.3K model have proven to be reliable dating tools when applied to Roman archaeological sites from Catalonia, in the NE corner of Spain (Gómez-Paccard and Beamud, 2008; Gómez-Paccard et al., 2013; Prevosti et al., 2013). However, a successful archaeomagnetic dating requires a minimum chronological context, usually inferred from archaeological evidence. This is due to the fact that a given value of the retrieved archaeomagnetic datum can occur at different time periods. In particular, magnetic inclination values for Iberia during the first five centuries AD are similar (Gómez-Paccard et al., 2013).

In this paper, we use archaeomagnetic data to constrain the age of last use of kilns at five archaeological sites from Catalonia (Fig. 1). Some of them are actually minor sites, they consist of only a single kiln and they lack of any datable artefacts. Despite their secondary significance, dating them is also important because archaeological sites must not be viewed as separate isolated entities but as a part of a mosaic that can reveal the history of a region.

* Corresponding author. Tel.: +34 935868365; fax: +34 935811263.
E-mail addresses: Lluis.Casas@uab.cat, Lluis.Casas@gmail.com (L. Casas).

0305-4403/$ – see front matter © 2013 Elsevier Ltd. All rights reserved.
http://dx.doi.org/10.1016/j.jas.2013.10.020

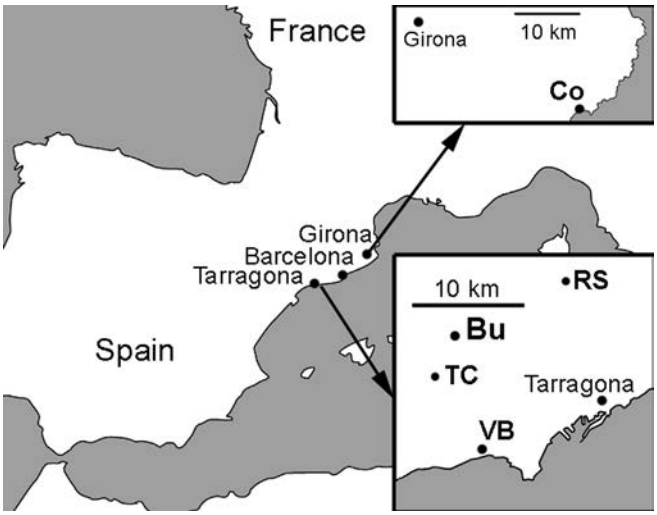

Fig. 1. Location of the sampled archaeological sites in Catalonia.

2. Archaeological background of the studied sites

2.1. Vil·la de Barenys (VB)

This Roman villa-type settlement was known from the mid-19th century and has been severely damaged during the 20th century due to gravel extraction works. In 2007 the remaining site was fully excavated (Otiña, 2009) and a kiln was found (Fig. 2). Once the excavations were completed and the kiln had been sampled archaeomagnetically, the area was developed as an archaeological park.

The kiln was circular with a diameter of about 2 m and it was built using the natural slope of the land. The firing chamber was completely covered by slag. The grid, the baking chamber and the stoke hole were also preserved. The grid was thick, slightly vaulted internally and with hollow pipes to allow the heated air into the baking chamber. There were no central or lateral pillars to hold the grid and therefore the kiln cannot be ascribed to any of the Cuomo di Caprio and Le Ny types. The stoke hole was opened in a wall made of *tegulae*. Next to the kiln there was a rectangular portico structure (its preserved area is 3.4 × 5 m) that was identified as a working area. The excavated infills of this area produced abundant slag, pottery wastes and other debris. The wastes are chronologically irrelevant except for Tarraconense amphorae Dressel 2–4 with a slightly evolved lip. This indicates that the abandonment of the structure was not before the third quarter of the 1st century AD (Járrega and Otiña, 2008), this chronology is confirmed by a dish lid, form Ostia III, 332 (Hayes, 1972). At the upper part of the site two dug structures were identified. These were perhaps related to clay extraction and later they were reused as waste dumps. Their infills were dated at the turn of the era. At the lower part of the site a similar dug structure produced *tegulae* and lots of firing rejects, among the *tegulae* the imprint of a *Pompeius* has been documented (Berni Millet, 2010).

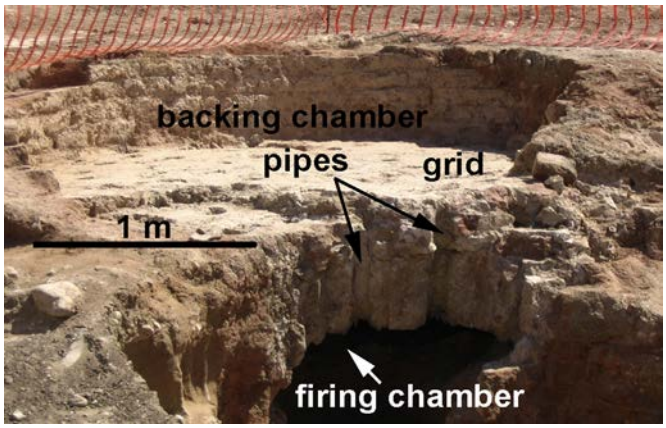

Fig. 2. Photograph of kiln VB at Vil·la de Barenys. The internal walls of the firing chamber were sampled on the whole perimeter.

2.2. La Buada (Bu)

This site locates in Reus (12 km north-east from Tarragona) and it was also already known in the late 19th century. Several archaeological field surveys were performed by amateur archaeologists during the first decade of the 20th century and also in its fifties and seventies, although the site has never been excavated. Recently, in 2008, the site was systematically surveyed (Prevosti and Abela, 2011) and an area of about 4.5 ha bearing great abundance of Roman pottery fragments was delimited. Besides pottery, some fragments of *opus signinum* pavement were also found. Two kilns were identified, as well as the remains of walls and several inhumations. One of the kilns has a cylindrical shape (Sanz, 1975) and at present is heavily damaged. The other kiln, better preserved, was sampled. Morphologically it can be included within Fletcher's (1965) Type 4A, Cuomo di Caprio's (1971) Type II/C or Le Ny's (1988) Type IIF, i.e. rectangular with a double passageway firing chamber (4.6 m wide) and a double row of arches that supported the clay pipe grid. The walls are made of adobe and mud that hardened in the first firing, the presently preserved height is ~2 m. It is located at field number 466 in Prevosti and Abela (2011) cut by a gully. Two arches (1.3 m wide each) of the system that supported the clay pipe grid are exposed (Fig. 3).

On field number 466 a large variety of pottery fragments were found including, among others, Iberian pottery, common ware (2nd and 1st centuries BC) and different types of amphorae (Iberian, Italic, Ebusitan, Betic and Tarraconense) and *terra sigillata* (Italic, south-Gaulish, Hispanic and African A, C and D). The local production was inferred by the identification of pottery wastes, these included Pascual 1 (50 BC–50 AD) and Dressel 2–4 (25 BC–300 AD) amphorae, *tegulae* and *antefixes*. The large variety of material indicates that the activity in the area lasted from the 2nd century BC to the late 5th century AD. However, taking into account de local production of amphorae (López Mullor and Martín, 2008), the chronology can possibly be restricted to the 1st, 2nd and 3rd centuries AD. Moreover, the stamps on Dressel 2–4 fragments from the site have been studied; Berni Millet (2010) reports CR (*in collo*) and IR (*in campana*) stamps. A parallel IR on Dressel 2–4 from Carthage gives a chronological horizon of the second quarter of the 1st century AD (Berni Millet, 2010).

To sum up, the occupation of the field originated during the Roman Republic period (late 2nd century BC) as indicated by Dressel 1A amphorae, its main period of activity would have been in the 1st and 2nd centuries AD and the activity lasted at least until the late 5th century as indicated by ARS form Hayes 91 (mid/late 5th century to mid-7th century AD). The site is interpreted as a Roman pottery workshop probably related to a villa.

2.3. Sota la Timba del Castellot (TC)

This is a big isolated kiln that appears cut (Fig. 4) by a trench in a footpath (*camí d'en Gaset*) south to the hill of La Timba del Castellot,

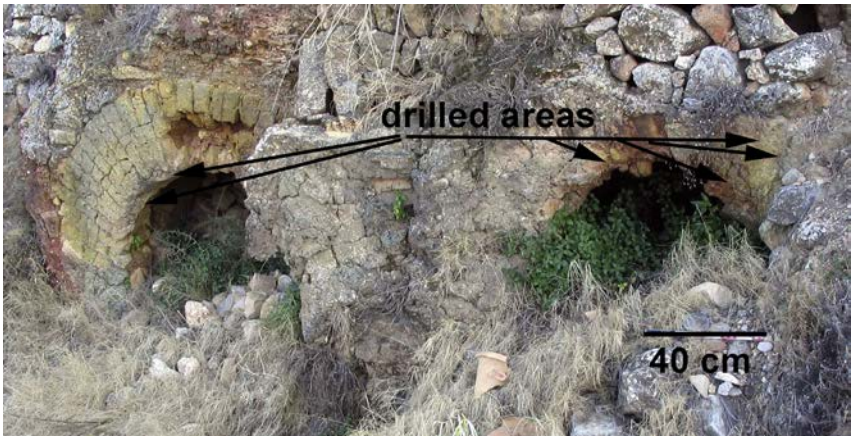

Fig. 3. Photograph of kiln Bu at La Buada with indication of the drilled areas below the arches that supported the grid.

in Riudoms (17 km east from Tarragona). The existence of this kiln had not been previously reported. It is very close to the Iberian settlement 'Timba del Castellot' (Arrayás, 2005) and even nearer to the Roman site of 'Sota la Timba del Castellot' (Berni Millet, 2010). The kiln walls are made of baked clay (black at the bottom and reddish towards the top). The bottom of the kiln was archaeomagnetically sampled. Typologically it consists of a single cylindrical (~2 m at the bottom and more than 2 m high) firing chamber similarly to traditional (medieval or modern) kilns to produce glue. However, the described typology is not exclusive of medieval and modern times, thus an older age cannot be ruled out. We performed a surface field survey that produced basically Iberian common ware and Italian amphorae fragments (among them Dressel 1A, late 2nd century BC). Fragments of Tarraconense amphora were also noticed, among them Dressel 2–4 (25 BC–300 AD) was identified. Finally, a fragment of African coarse ware (Lamboglia 10) with slip remains was also found. It is worth to mention that a fragment of Iberian common ware (2nd–1st centuries BC) was found among the exposed kiln filling. The ensemble of datable fragments suggests a chronology ranging from the late 2nd century BC to the early 2nd century AD.

2.4. Riera de la Selva (RS)

The inferior part of a kiln appeared after erosion in the left margin of the *Riera de la Selva* stream due to heavy rains in Vilallonga del Camp, 11 km north from Tarragona. The kiln was first reported quite recently (Járrega and Prevosti, 2011); the exposed remains (Fig. 5) correspond to the subterranean fire box and a wall made of bricks that divides it into two. This wall was archaeomagnetically sampled. The kiln has a Roman typology, Cuomo di Caprio II/c or Le Ny's IIF, rectangular with a double passageway firing chamber (Cuomo di Caprio, 1971) and arches, presently

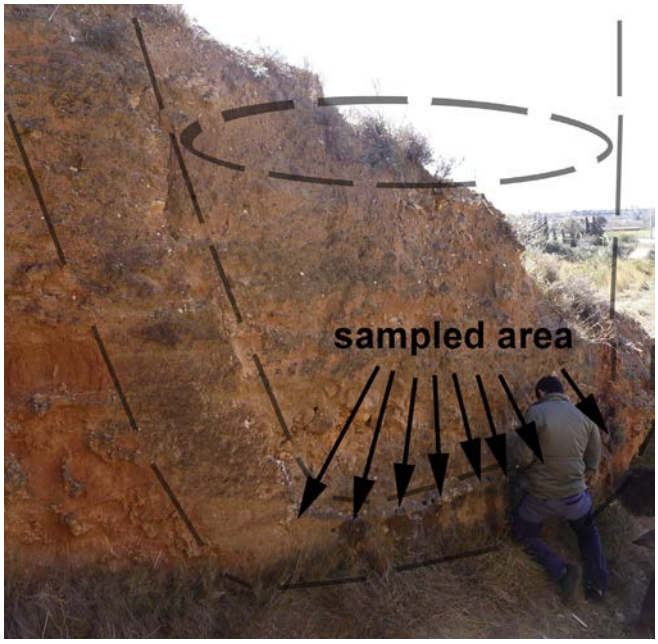

Fig. 4. Photograph of the sectioned kiln TC at Sota la Timba del Castellot. Sampling was performed at the bottom of the structure. A sketch of the kiln has been drawn on the picture.

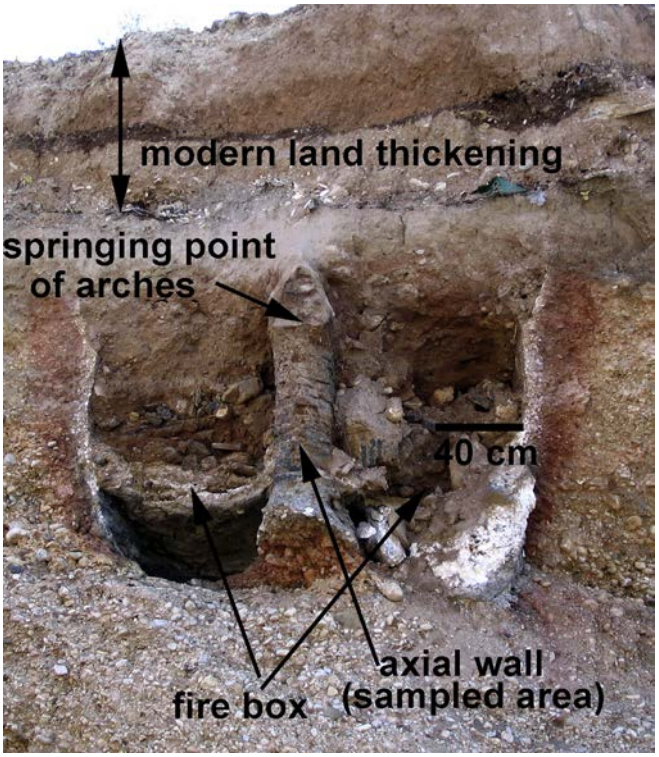

Fig. 5. Photograph of the sectioned kiln RS at Riera de la Selva. Sampling proceed on the left side of the axial wall.

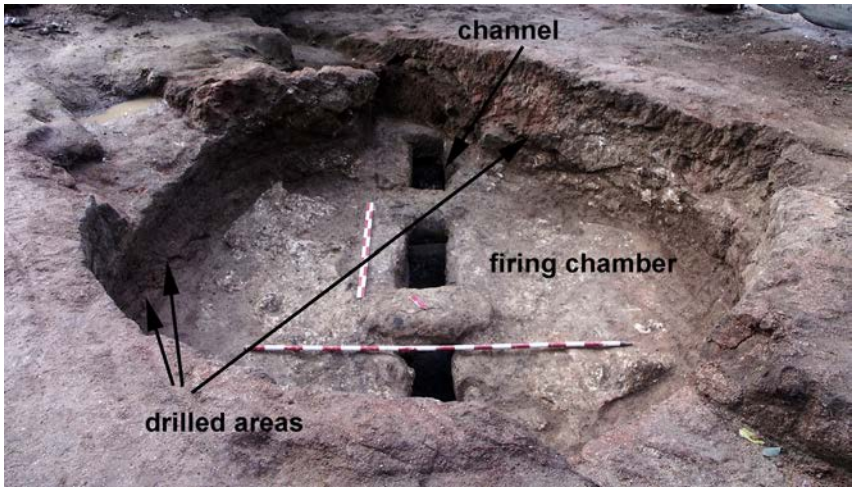

Fig. 6. Photograph of kiln Co at Collet de Sant Antoni de Calonge with indication of the sampled areas (courtesy of X. Aguelo).

missing, to support the grid. The kiln was excavated in the slope of the stream, so the side walls did not require bricks. No typologically datable pottery fragments were found inside the exposed kiln, where only a few *imbrices* or similar roof tiles were identified. The land above the kiln show evidences of modern thickening and leveling up.

2.5. Collet de Sant Antoni de Calonge (Co)

Collet is an elongated hill near Sant Antoni de Calonge, in the Costa Brava (some 25 km south-east from Girona). The site is known by a Roman villa and a complete large pottery workshop with several kilns that were excavated from 2000 in the lower part of the hill, to the north and east (Nolla et al., 2004). The workshop produced Pascual 1 and Dressel 2–4 amphorae, common ware, building material and large *dolia*. The pottery and coins retrieved from the workshop date it between late 1st century BC and the 1st century AD.

In 2008 an excavation some 150 m away from the main site, in the southern slope of hill, revealed a circular lime kiln (Fig. 6) with a diameter of 3.2 m and a stoke hole to the south (Aguelo, 2010). The kiln was dug in the natural granitic ground and it was archaeomagnetically sampled. A small channel was dug on the kiln's floor with three quadrangular openings to clean it. The grid was found collapsed and it was originally held by two pillars. Despite not being a pottery kiln it can typologically be classified as a two-pillar version of the Cuomo di Caprio's (2007) type I/A. The retrieved fragments from the kiln infills were basically unidentifiable except for a lip of Pascual 1 amphorae. This would indicate an age of late-1st century BC (López Mullor and Martín, 2008).

3. Archaeomagnetic directions

3.1. Materials and methods

Oriented cylindrical cores (~2.5 cm diameter) were collected from the internal walls of the five kilns using a portable electrical drill with a water-cooled diamond bit, following the standard palaeomagnetic sampling procedure. The in-situ azimuth and dip of the drilled holes were measured using a compass coupled to a core orienting fixture. The nature of the sampled materials is different for each kiln: baked adobe and clay (Bu), baked clay (TC), bricks (RS), slag and baked adobe (VB) and oxidized granite (Co). All the sampled materials present clear evidence of exposure to intense heat during firing.

Each sample produced a single specimen except one sample from RS that produced two. A stored archaeomagnetic direction was obtained for each specimen. The analyses included stepwise demagnetization of the natural remanent magnetization (NRM) and measurement of the magnetization left after each step. Schoenstedt TSD-1 and Magnetic Measurements MMTD-80 thermal demagnetizers and 2G Enterprises superconducting rock magnetetometer were used. All this equipment is available at the Paleomagnetic Laboratory of Barcelona, SCT UB-CSIC. The obtained results were analyzed as described in Prevosti et al. (2013), the characteristic remanent magnetization (ChRM) directions were calculated by principal component analyses (Kirschvink, 1980) on Zijderveld diagrams and the corresponding maximum angular deviation (MAD) was calculated. Specimens with MAD values higher than five were disregarded (Hervé et al., 2011). Mean directions for each kiln were computed following Fisher (1953) statistics; concentration parameter k and confidence factor α_{95} were also computed. The obtained mean directions were compared both with the SCHA.DIF.3K model (Pavón-Carrasco et al., 2009) and the SVC for the Iberian Peninsula (Gómez-Paccard et al., 2006a) using a Matlab dating tool developed by Pavón-Carrasco et al. (2011).

3.2. Results

Representative Zijderveld diagrams of specimens from each kiln are shown in Fig. 7 along with the stereographic projections of all the individual ChRM directions grouped by site. A total of 72 specimens were measured from five kilns. Only six specimens were rejected due to MAD $>5^\circ$ (one from TC, two from RS and three from Co). However, it is worth to mention that five Co specimens produced MAD values $>4^\circ$. Besides that, three samples were also rejected due to inconsistent archaeomagnetic directions (one from VB attributable to an incorrect replacement of a broken core and two from RS possibly due to a not in situ sampling point). Table 1 summarizes the archaeomagnetic directional results.

Probability density functions of possible dates for declination and inclination were obtained comparing the results with both the SCHA.DIF.3K model (Fig. 8) and the SVC for the Iberian Peninsula; the latter implied the relocation of the data to Madrid. The probability functions were combined to obtain the most probable dating solutions at 95% confidence level (Figs. 8 and 9). These distributions generally indicate several time intervals, some of them lie near or

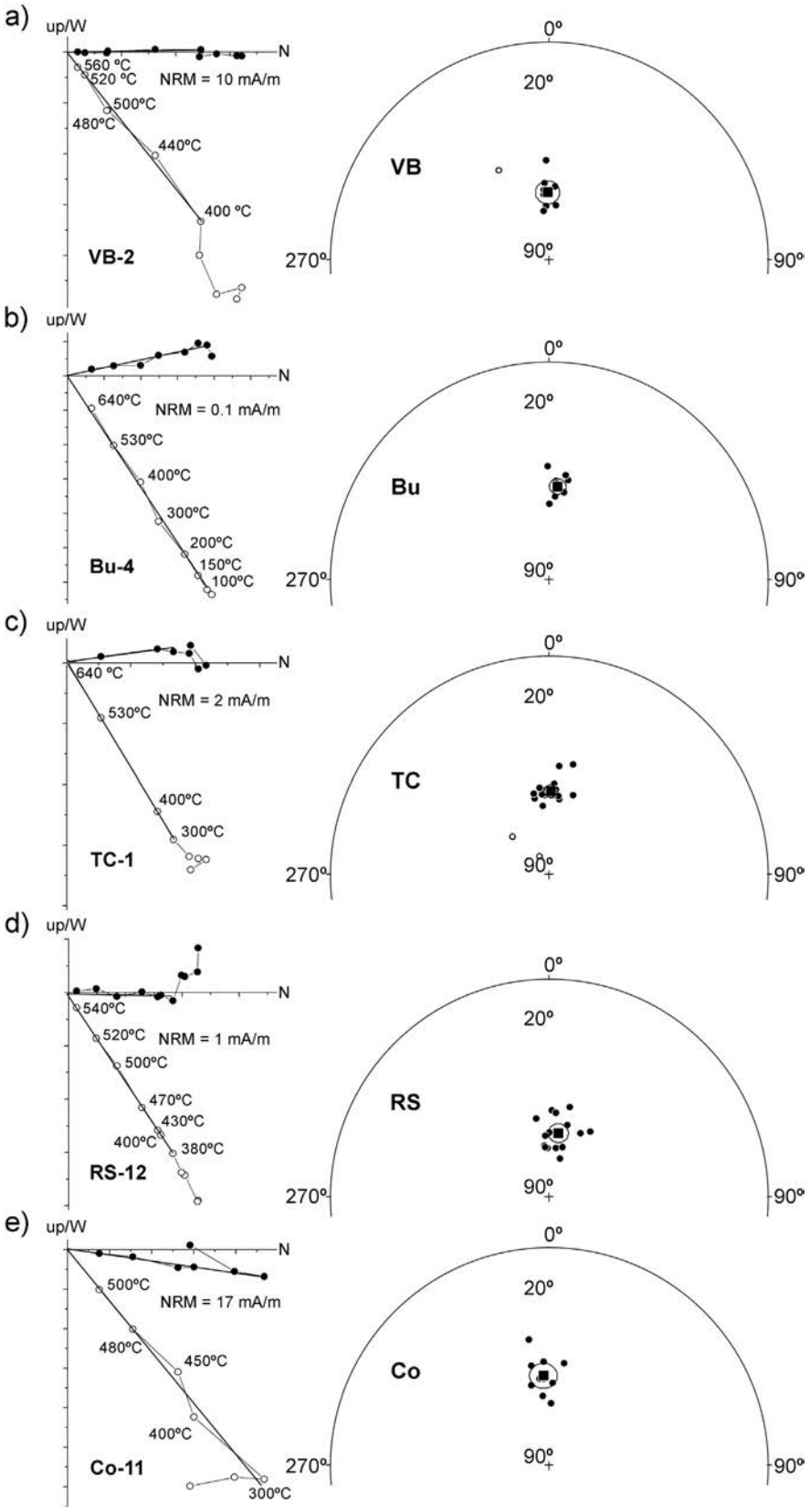

Fig. 7. To the left, a representative Zijderveld plot for a specimen from each sampled kiln (left) depicting the orthogonal projection of the remanent magnetization vectors during progressive demagnetization; lines indicate the ChRM directions. To the right, stereographic projection of the archaeomagnetic directions calculated for each sample from (a) VB, (b) Bu, (c) TC (d) RS and (e) Co kilns; open solid symbols correspond to directions not used to compute mean directions and the squares are the obtained mean directions with concentric α_{95} error circles.

Table 1
Coordinates of the sampled sites (Lat., latitude and Long., longitude), sample labels and number of collected samples; n is the number of standard specimens obtained from the N collected samples; n_u is the number of specimens used to compute the archaeomagnetic direction; D, archaeomagnetic declination; I, archaeomagnetic inclination; k and α_{95}, precision parameter and 95% confidence limit of the characteristic remanent magnetization, from Fisher statistics.

Site	Lat. (°N)	Long. (°E)	Label	n/N	n_u	D (°)	I (°)	k	α_{95} (°)
Vil·la de Barenys	41.08	1.12	VB	9/9	8	358.9	64.5	159.2	4.4
La Buada	41.17	1.09	Bu	10/10	10	5.3	54.5	264.6	3.0
Sota la Timba del Castellot	41.14	1.07	TC	20/20	19	1.2	58.5	207.5	2.3
Riera de la Selva	41.22	1.18	RS	20/19	16	8.4	65.7	106.4	3.6
Collet de Sant Antoni de Calonge	41.85	3.11	Co	13/13	10	356.5	56.0	97.9	4.9

within the presumed archaeological ages, and others do not (Table 2).

3.3. Discussion

From the five studied kilns, one of them (Co) has a well constrained age by archaeological evidence, BC 25–1. In contrast, VB and Bu kilns have a less constrained archaeological age, BC 50–AD 75 and AD 1–300 respectively, and kilns TC and RS have a very imperfectly determined archaeological age. For all the kilns, the archaeomagnetic directions bring data to discuss their actual age.

According to the probability density function, the last use of kiln Co would be slightly later than indicated by archaeological hypotheses. This kiln would have been used at least at the very end of the 1st century BC (actually within the presumed archaeological age) or the first quarter of 1st century AD, depending on whether the SCHA.DIF.3K model or the Iberian SVC data is used.

For the kiln in Vil·la de Barenys (VB) the last use of the kiln appears to be within the older segment of the time interval corresponding to the presumed archaeological age. This corresponds to a time period within the 1st century BC and, at a 95% confidence level, not within the 1st century AD. The probability density distribution indicates also a possible last use within the Common Era, but this could not be before the 5th century (according to SCHA.DIF.3K model, Fig. 8a) or the 6th century (according to the Iberian SVC, Fig. 9a) and thus, quite far from the presumed archaeological age though not excludable.

In the case of the kiln in La Buada, (Bu) archaeomagnetic data indicate a last use of the kiln fully compatible with the presumed archaeological age. This would have been at least up to the end of the 1st century AD or early 2nd century AD. The Iberian SVC produces a seemingly worse probability distribution because the obtained result concentrates a very small amount of probability within the plausible time range compared with the main probability peak centered around year 1500 AD (Fig. 9b), which is an age not archaeologically supported.

The correspondence between the presumed archaeological ages based on archaeological hypotheses and part of the probability density distributions inferred from archaeomagnetic direction dating reflects the applicability of both SCHA.DIF.3K and the Iberian SVC dating tools. This applicability had already been attested in NE Spain (Prevosti et al., 2013). This allows us to discuss the results from archaeological sites that almost lack of datable artefacts (like TC and RS).

The probability density distribution obtained for the isolated kiln in Sota la Timba del Castellot (TC) is compatible with both Iberian and Roman periods. In contrast, the medieval or modern hypotheses are definitely rejected using the SCHA.DIF.3K model and restricted to the AD 1549–1629 interval using the Iberian SVC. Taking into account the few datable fragments recovered on the surface of the site we suggest that the most plausible time intervals of last use for kiln TC are BC 155–75 and BC 34–AD 158 (using SCHA.DIF.3K) or BC 74–AD 109 (using the Iberian SVC).

The isolated kiln in Riera de la Selva (RS) is typologically Roman but the archaeomagnetic data point to late Antiquity (the oldest possible age would be the 6th century). We carefully checked the verticality of the kiln walls to identify moves of the whole kiln structure that would invalidate this conclusion. However, no hints of such shift were found. A rotation on a horizontal plane cannot be excluded but this movement would be rather improbable. Once accepted, the archaeomagnetic result constitutes an evidence of the survival of the kilns of Roman type (Cuomo di Caprio II/c or Le Ny IIF) up to late Antiquity.

4. Rock magnetism and archaeointensities

4.1. Materials and methods

Archaeointensity determinations require stable non-interacting single domain (SD) or pseudo-single domain (PSD) remanence carriers and thus, rock magnetism properties must be analyzed before attempting intensity measurements. Samples from three kilns were collected to perform both rock magnetism and archaeointensity measurements. These kilns were Bu, TC and RS, whose archaeomagnetic directions were more uniform and presented the smallest α_{95} values (Table 1). Fragments from their internal walls could be removed and drilled in the laboratory to produce standard palaeomagnetic cores (nine from Bu kiln, nineteen from TC kilns and twenty-three from RS kiln). The spare material was crushed and kept to perform magnetic analyses.

Magnetic analyses were performed at the Geomagnetism Laboratory, University of Liverpool. These included susceptibility measurements from liquid nitrogen to room temperature in a MS2 magnetic susceptibility meter from Bartington and hysteresis properties, isothermal remanent magnetization (IRM) acquisition, remanence coercivity and magnetization versus temperature curves measured in a Magnetic Measurements variable field translation balance (VFTB). VFTB results were analyzed using RockMagAnalyzer 1.0 software (Leonhardt, 2006). Archaeointensity analyses were carried out at the Paleomagnetic Laboratory of Barcelona, SCT UB-CSIC, according to the Coe variant of a Thellier-type experiment (Coe, 1967) as described in Prevosti et al. (2013). Cooling rate tests were performed at 580 °C on all samples following the procedure described in Chauvin et al. (2000). The obtained correction factor was only applied for samples with stable acquisition capacity ($r_2 < 5\%$ where $r_2 = (TRM_1 - TRM_3)/TRM_1$). For the rest of the samples an arbitrary correction of −5% was applied (Gómez-Paccard et al., 2013). Quality control criteria for the obtained archaeointensities and computation of overall intensity values for each analyzed were applied as Prevosti et al. (2013). The obtained archaeointensity estimates were compared both with the SCHA.DIF.3K model (Pavón-Carrasco et al., 2009) and the Bayesian SVC for western Europe (Gómez-Paccard and Beamud, 2008).

4.2. Rock magnetic results

Magnetic domain state can be estimated using the classical Day plot (Day et al., 1977), all the measured samples lie within the PSD region. Statistically, most of TC samples group at the top left corner

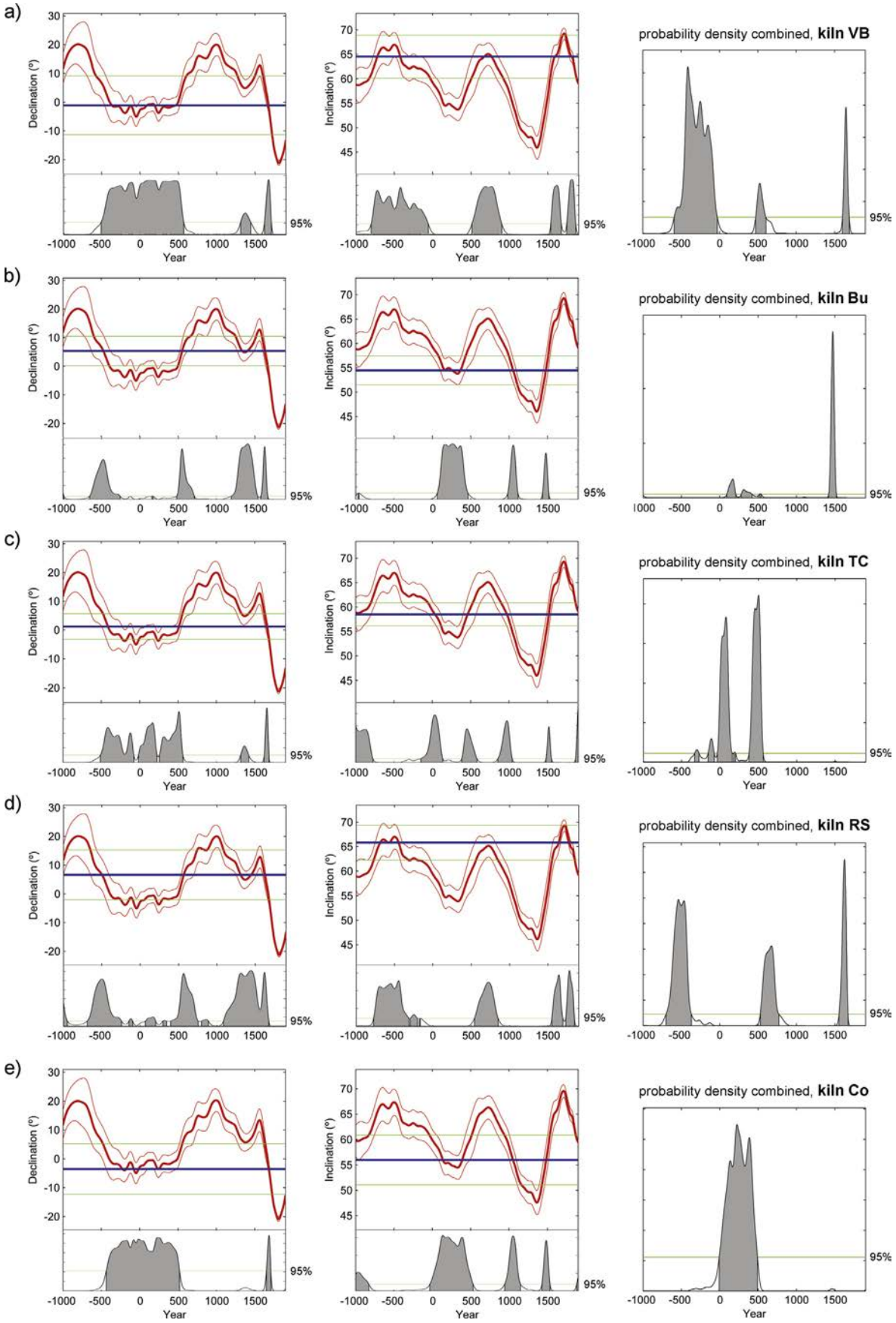

Fig. 8. Probability-of-age density functions obtained with the Matlab tool from Pavón-Carrasco et al. (2011) for (a) VB, (b) Bu, (c) TC, (d) RS and (e) Co kilns, using SCHA.DIF.3K model.

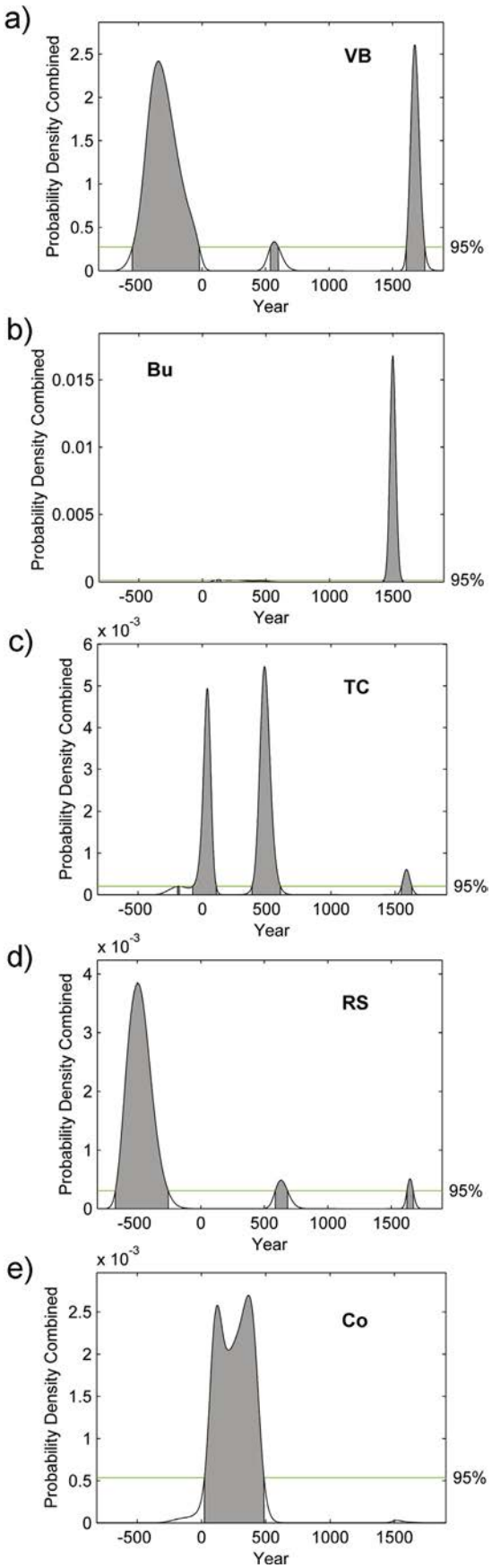

Fig. 9. Combined (declination and inclination) probability-of-age density functions obtained with the Matlab tool from Pavón-Carrasco et al. (2011) for (a) VB, (b) Bu, (c) TC, (d) RS and (e) Co kilns, using the Iberian SVC. Archaeomagnetic directions were relocated to Madrid.

Table 2
Archaeomagnetic ages comparing the archaeomagnetic directions with SCHA.DIF.3K model and the Iberian SVC. Presumed ages according to archaeological evidence are listed for comparison.

Kiln	Main solutions at 95% confidence level.		Presumed archaeological age
	SCHA.DIF.3K	Iberian SVC	
VB	BC 591–28 AD 472–604 AD 1603–1691	BC 548–22 AD 539–600 AD 1608–1754	BC 50–AD 75
Bu	AD 92–209 AD 280–421 AD 520–540 AD 1419–1521	AD 114–146 AD 1430–1573	AD 1–300
TC	BC 330–274 BC 155–75 BC 34–AD 158 AD 177–202 AD 378–563	BC 192–179 BC 74–AD 109 AD 387–607 AD 1549–1629	BC 125–AD 125 /Medieval?/Modern?
RS	BC 699–382 AD 538–758 AD 1567–1692	BC 695–286 AD 582–719 AD 1628–1652	Roman?
Co	BC 7–AD 492	AD 24–486	BC 25–1

of that region (close to the SD region) whereas RS and Bu samples lie in the central PSD region and sometimes towards its bottom right corner (close to the multidomain (MD) region). However, to assume that all the analyzed samples consist in an assembly of PSD particles could be an oversimplified conclusion. There are several indicators that point to a more complex assemblage. On one hand, all the recorded hysteresis loops (Fig. 10a) have slouching shoulders with shape parameters σ_{hys} (Fabian, 2003) ranging from −0.35 (for a RS sample) to −0.89 (for a TC sample). Potbellied loops indicate at least two different magnetic populations that could consist of superparamagnetic (SP) and SD particles (Tauxe et al., 1996). Indeed, simulations of the obtained hysteresis loops required at least two magnetic components besides the paramagnetic contribution. However, plots of σ_{hys} versus E_t^{Δ}/E_{hys} (inferred from B_{rh}/B_{cr} ratios) point clearly to a MD assembly (Fabian, 2003) for most of Bu and RS samples, and to particles within the SD–MD transition zone for TC samples. To add complexity, all thermomagnetic curves indicate a wide distribution of blocking temperatures without clear magnetic transition values (Fig. 10b) although the thermal reversibility is good. Finally, almost all low temperature susceptibility dependence plots exhibit hints of the Verwey transition (Fig. 10c) which is indicative of low-Ti titanomagnetites in MD state (Moskowitz, 1980). Taking into account the difficulty to elucidate the exact nature of the magnetic mineralogy of the samples from the three analyzed kilns, we decided to attempt archaeointensity determinations for all the samples. This allows, at least, a check of the homogeneity of the stored values.

4.3. Archaeointensities and discussion

The success rate for archaeointensity measurements has been very variable. Only one sample from kiln Bu failed, due to *f* fraction lower than 0.5. For samples from kiln TC five measurements produced convex-down Arai plots (e.g. TC-i2b in Fig. 11b) and thus their archaeointensity values were not obtainable by standard methods (Dunlop et al., 2005), three more TC samples failed due to low *f* fractions. Finally all twenty-three archaeointensity measurements on RS samples failed due to non-linear Arai plots (e.g. RS-i7

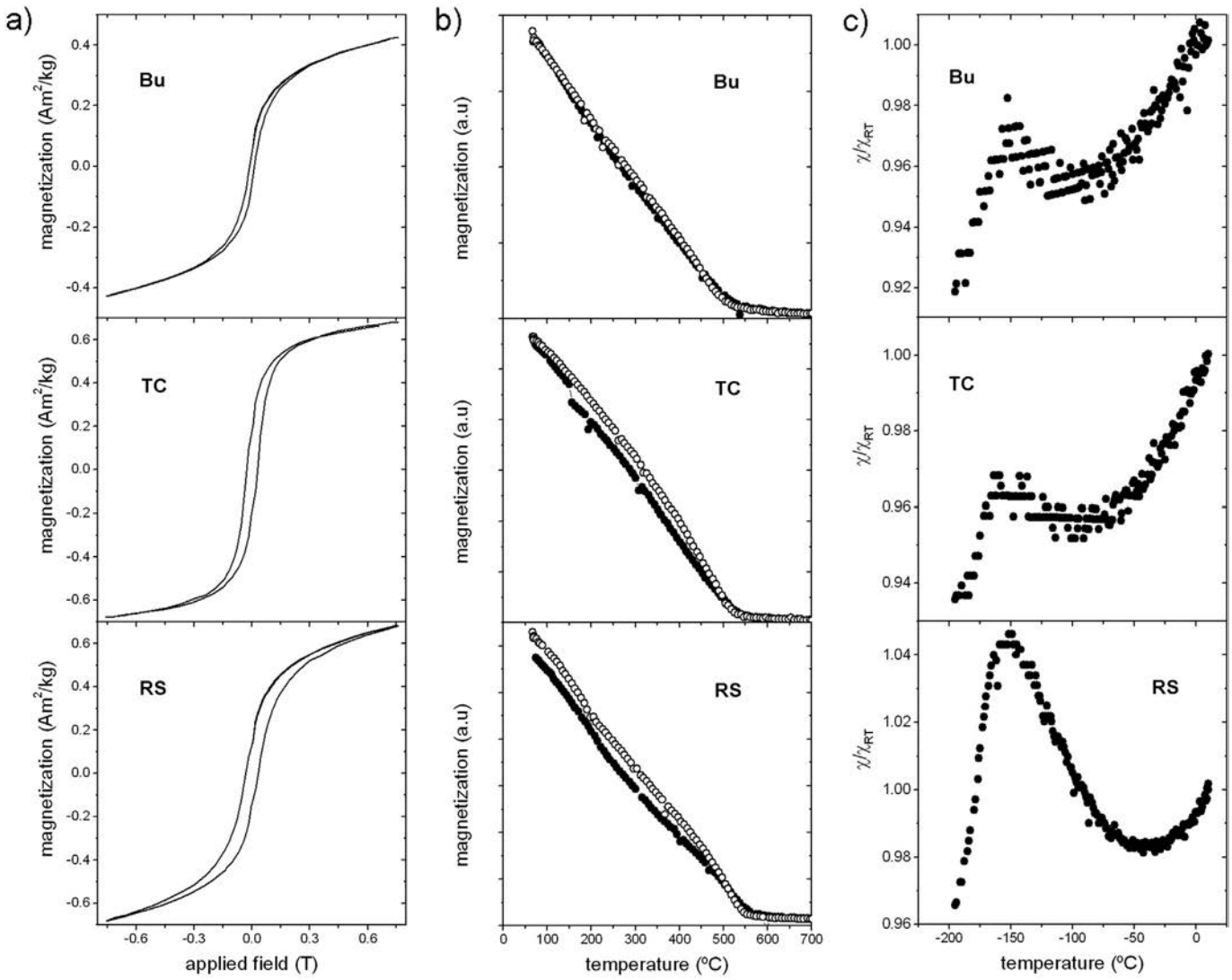

Fig. 10. Representative rock magnetic results from Bu, TC and RS kilns. (a) Hysteresis loops, (b) thermomagnetic curves and (c) low temperature susceptibility dependence.

in Fig. 11b) and therefore no archaeointensity estimates were obtained for kiln RS.

All the measurements that produced linear Arai plots with f fractions >0.5 and positive pTRM checks are listed in Table 3 (for Bu samples) and Table 4 (for TC samples). Representative Arai plots of specimens from kilns Bu and TC are shown in Fig. 11a. The individual archaeointensity estimates were added up observing the specimen-sample hierarchy to obtain an overall estimate for each kiln (Fig. 12). All estimates from Table 4 were taken into account to compute the overall archaeointensity for kiln TC (61.5 ± 9.2 μT). In contrast, the anomalously low archaeointensity from sample Bu-i6 (Fig. 11b) was excluded from the computation of the archaeointensity for kiln Bu (57.7 ± 6.1 μT).

Despite the relatively large uncertainties of the obtained archaeointensity estimates, the values for Bu and TC kilns can be used respectively as a new reference value and to constrain further the age of the kiln. La Buada is one of the sites with a constrained age by archaeological evidence (AD 0–300) consistent with the archaeodirectional dating of the last use of its investigated kiln (end of the 1st century AD or early 2nd century AD onwards). The intersection between the archaeological and the archaeodirectional dating produces an age (AD 100–300) that can be associated to the obtained archaeointensity as a new reference point to be used for future refinements of the dating tools. Taking the errors into account, the new archaeointensity point is very consistent with the SCHA.DIF.3K model prediction and slightly lower than the one predicted by the western European intensity SVC (Fig. 13). The intensity value obtained for kiln TC reconfirm the Roman age suggested previously (see Section 3.3). The medieval or modern hypotheses can practically be discarded as indicated by the combined (declination, inclination and intensity) probability density distributions that were obtained using the SCHA.DIF.3K model (Fig. 14a) and the Iberian SVC combined with the western European intensity SVC (Fig. 14b). Both distributions are bimodal with a peak centered at the turn of the Common Era and another centered at the 5th century (using SCHA.DIF.3K) or at the 6th century (using the SVCs).

5. Conclusions

New archaeomagnetic data have been obtained for five kilns from NE Spain, including two full-vector data. The age of last use of these kilns has been constrained using archaeomagnetic dating tools. The obtained time intervals roughly agree with the

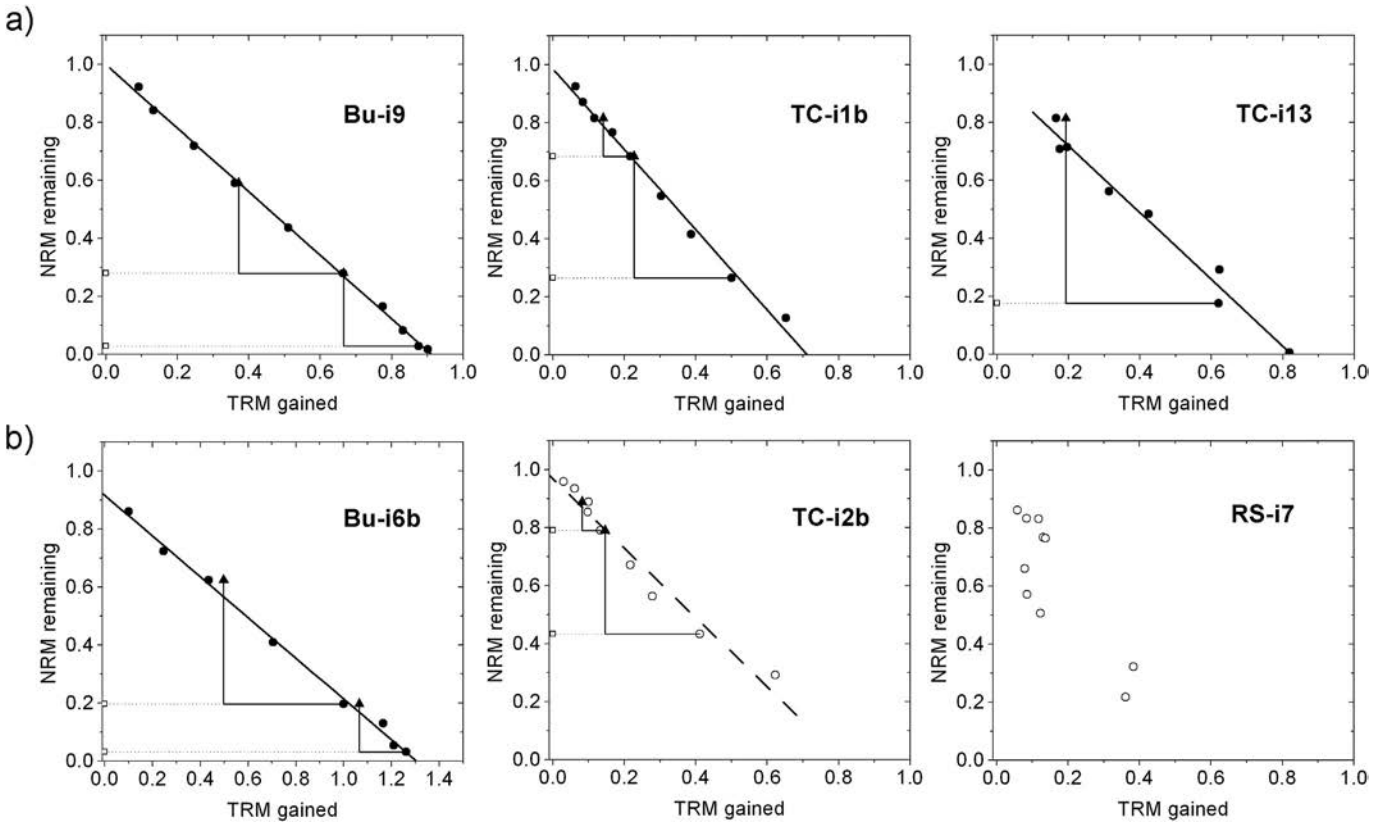

Fig. 11. (a) Representative Arai plots of normalized NRM remaining against TRM gained for specimens from kilns Bu and TC. (b) Anomalous low intensity recorded in a Bu specimen, convex-down Arai plot of a TC specimen and non-linear Arai plot of a RS specimen.

chronological interpretations inferred from archaeological evidence: i) in Collet de Sant Antoni (Co) the magnetic data indicate a slightly later age; ii) in Vil·la de Barenys (VB) the age has been constrained within the 1st century BC and iii) in La Buada (Bu) the age has been constrained within the 2nd–3rd centuries AD and an archaeointensity value has been associated to this time interval. Isolated kilns without precise presumed archaeological age have also been dated. For the kiln at Sota la Timba del Castellot (TC) ages either at the turn of the Common Era or within 5th–6th century are suggested. The kiln at Riera de la Selva (RS) would have been last used during the 6th century AD or later, this result constitutes an evidence of the survival of the kilns of Roman type (Cuomo di Caprio II/c or Le Ny IIF) up to late Antiquity.

Table 3
Archaeomagnetic intensity results for kiln Bu obtained from linear Arai plots with *f* fractions >0.5 and positive pTRM checks. All samples except Bu-i6 (anomalous low intensity) were used to compute the mean intensity value.

Specimen	F (μT)	F_{CR} (μT)	σ (μT)	N	f	g	q
Bu-i1	63.0	59.8	2.5	9	0.87	0.83	24.8
Bu-i2	63.2	60.0	3.9	8	0.74	0.83	16.2
Bu-i3	62.8	59.7	3.6	7	0.76	0.80	17.4
Bu-i5	56.8	54.0	7.5	7	0.50	0.79	7.6
Bu-i6a	37.7	35.8	1.4	7	0.83	0.78	25.9
Bu-i6b	35.1	33.4	1.2	8	0.83	0.81	29.0
Bu-i7	55.4	52.6	3.3	8	0.88	0.84	16.9
Bu-i8	65.9	62.6	2.3	10	0.91	0.87	28.1
Bu-i9	54.8	52.1	0.9	10	0.90	0.87	60.0
Mean value 57.7 ± 6.1							

Columns from left to right: Specimen, label of the specimen identifying the kiln (Bu) and the core number; F, raw intensity; F_{CR}, cooling rate corrected intensity; σ, standard deviation of the intensity estimate; N, number of heating steps used for the intensity determination; f, fraction of NRM used for intensity determination; g, gap factor and q, quality factor as defined by Coe (1967).

Table 4
Archaeomagnetic intensity results for kiln TC obtained from linear Arai plots with *f* fractions >0.5 and positive pTRM checks. All samples were used to compute the mean intensity value.

Specimen	F (μT)	F_{CR} (μT)	σ (μT)	N	f	g	q
TC-i1a	72.9	69.2	2.1	9	0.82	0.85	33.1
TC-i1b	69.5	66.0	3.3	9	0.80	0.85	19.8
TC-i9	55.4	52.6	14.1	8	0.50	0.77	3.9
TC-i10	65.0	61.7	18.4	7	0.56	0.80	3.5
TC-i12	57.2	56.9	16.2	6	0.57	0.73	3.5
TC-i13	59.8	60.4	5.6	7	0.81	0.75	10.8
TC-i16	60.2	58.7	13.4	7	0.74	0.79	4.5
TC-i17	58.1	55.2	4.9	8	0.77	0.75	10.7
TC-i18	63.9	63.0	6.1	9	0.77	0.76	10.3
TC-i19	65.8	64.2	5.9	9	0.80	0.72	11.2
Mean value 61.5 ± 9.2							

Columns from left to right: Specimen, label of the specimen identifying the kiln (TC) and the core number; F, raw intensity; F_{CR}, cooling rate corrected intensity; σ, standard deviation of the intensity estimate; N, number of heating steps used for the intensity determination; f, fraction of NRM used for intensity determination; g, gap factor and q, quality factor as defined by Coe (1967).

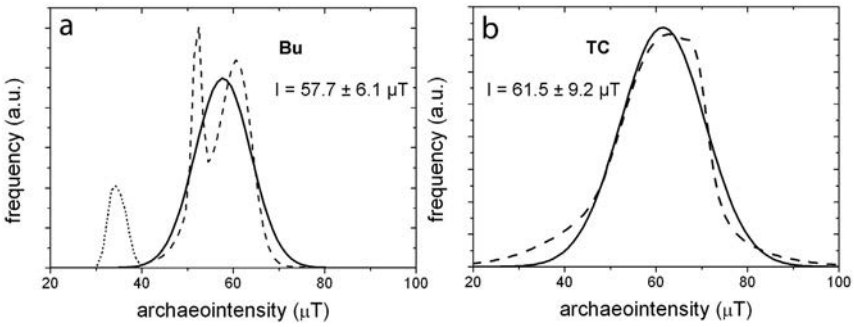

Fig. 12. Computation of mean archaeointensities for kilns Bu (a) and TC (b). The dashed line is the sum of all the individual results used to obtain the mean archaeointensity values by fitting to them a Gaussian curve (solid line). The dotted line in (a) corresponds to the anomalously low values obtained for Bu-i6 specimens.

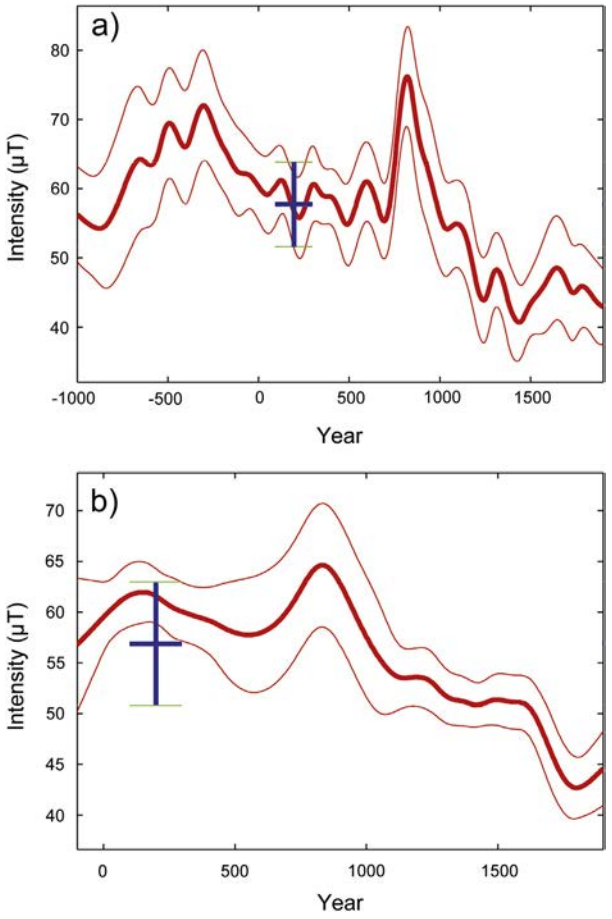

Fig. 13. A comparison of the archaeointensity obtained for kiln Bu with geomagnetic model SCHA.DIF.3K predictions (a) and the archaeointensity curve for western Europe (b).

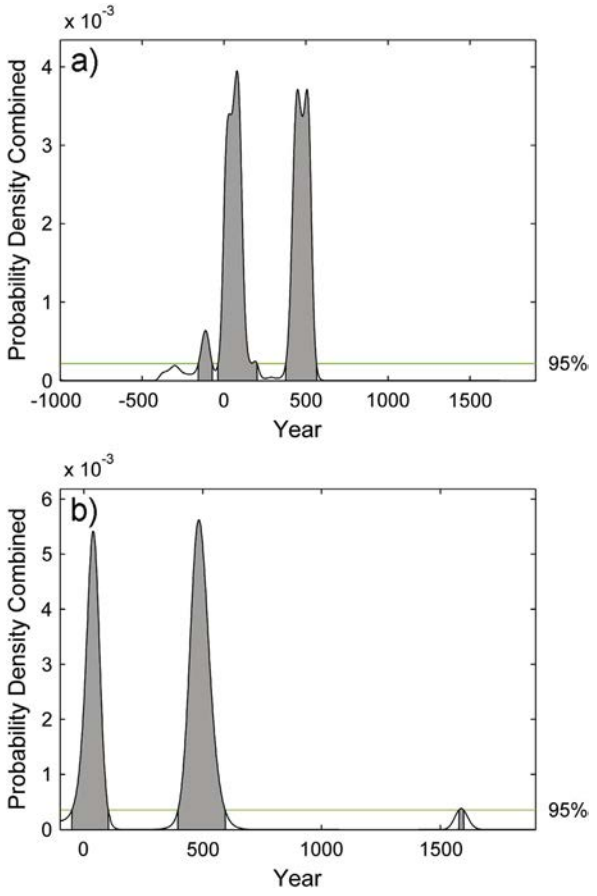

Fig. 14. Combined (declination, inclination and intensity) probability-of-age density functions obtained with the Matlab tool from Pavón-Carrasco et al. (2011) for kiln TC using the SCHA.DIF.3K model (a) and the direction Iberian SVC and the western Europe intensity SVC (b).

Acknowledgments

We are grateful to Xavier Aguelo for authorizing sampling on Collet de Sant Antoni and providing photographs of the sampled kiln. We thank Eugènia Estop, Marta Moreno and Àfrica Pitarch for their support during field work. We also would like to acknowledge two anonymous reviewers for their helpful and insightful comments. This research was funded by the Spanish Ministerio de Ciencia e Innovación (Project HAR2010-16953) and the Agencia Española de Cooperación Internacional para el Desarrollo (Spain-Tunisia bilateral project A1/039844/11).

References

Aguelo, X., 2010. Intervenció Arqueològica al Collet de Sant Antoni (Calonge, Baix Empordà). In: Grau Salvà, J., Prados Muñoz, A. (Eds.), X Jornades d'Arqueologia de les comarques de Girona (Arbúcies, 28–29 mai 2010), pp. 309–311.

Arrayás, M., 2005. Morfología del territorio de Tarraco (ss. III-I a.C.). Universitat de Barcelona, Barcelona.

Berni Millet, P., 2010. Epigrafia sobre *amphorae, tegulae, imbrex* i *dolia* a l'àrea occidental del Camp de Tarragona/epigraphy on *amphorae*, *tegulae*, *imbrex* and *dolia* in the western area of the Camp of Tarragona. Tarragona. In: Gorostidi, D. (Ed.), Ager Tarraconenis 3. Les inscripcions romanes/The Roman Inscriptions, Documenta 16, pp. 153–210.

Chauvin, A., Garcia, Y., Lanos, P., Laubenheimer, F., 2000. Paleointensity of the geomagnetic field recovered on archaeomagnetic sites from France. Phys. Earth Planet. Inter. 120, 111–136.
Coe, R.S., 1967. Paleo-intensities of Earth's magnetic field determined from tertiary and quaternary rocks. J. Geophys. Res. 72, 3247–3262.
Cuomo di Caprio, N., 2007. La ceramica in archeologia, 2: antiche tecniche di lavorazione e moderni metodi di indagine. L'Erma di Bretschneider.
Cuomo di Caprio, N., 1971. Proposta di classificazione delle fornaci delle fornaci per ceramica e laterizi nell'area italiana. Sibrium, pp. 371–464.
Day, R., Fuller, M., Schmidt, V.A., 1977. Hysteresis properties of titanomagnetites: grain-size and compositional dependence. Phys. Earth Planet. Inter. 13, 260–267.
Dunlop, D.J., Zhang, B., Özdemir, Ö., 2005. Linear and nonlinear Thellier paleointensity behavior of natural minerals. J. Geophys. Res. Solid Earth 110, B01103. http://dx.doi.org/10.1029/2004JB003095.
Fabian, K., 2003. Some additional parameters to estimate domain state from isothermal magnetization measurements. Earth Planet. Sci. Lett. 213, 337–345.
Fanjat, G., Aidona, E., Kondopoulou, D., Camps, P., Rathossi, C., Poidras, T., 2013. Archaeointensities in Greece during the Neolithic period: new insights into material selection and secular variation curve. Phys. Earth Planet. Inter. 215, 29–42.
Fisher, R., 1953. Dispersion on a sphere. Proc. R. Soc. London. Ser. A. Math. Phys. Sci. 217, 295–305.
Fletcher, D., 1965. Tipología de los hornos romanos de España. Arch. Esp. Arqueol. 38, 170–174.
Gómez-Paccard, M., Chauvin, A., Lanos, P., McIntosh, G., Osete, M.L., Catanzariti, G., et al., 2006a. First archaeomagnetic secular variation curve for the Iberian Peninsula: comparison with other data from western Europe and with global geomagnetic field models. Geochem. Geophys. Geosyst. 7, Q12001.
Gómez-Paccard, M., Catanzariti, G., Ruiz-Martínez, V.C., McIntosh, G., Núñez, J.I., Osete, M.L., et al., 2006b. A catalogue of Spanish archaeomagnetic data. Geophys. J. Int. 166, 1125–1143.
Gómez-Paccard, M., Beamud, E., 2008. Recent achievements in archaeomagnetic dating in the Iberian Peninsula: application to Roman and Mediaeval Spanish structures. J. Archaeol. Sci. 35, 1389–1398.
Gómez-Paccard, M., Beamud, E., McIntosh, G., Larrasoaña, J.C., 2013. New archaeomagnetic data recovered from the study of three Roman kilns from north-east Spain: a contribution to the Iberian palaeosecular variation curve. Archaeometry 55, 159–177.
Hayes, J.W., 1972. Late Roman Pottery. The British School at Rome, London.
Hervé, G., Schnepp, E., Chauvin, A., Lanos, P., Nowaczyk, N., 2011. Archaeomagnetic results on three Early Iron Age salt-kilns from Moyenvic (France). Geophys. J. Int. 185, 144–156.
Járrega, R., Otiña, P., 2008. Un tipo de ánfora tarraconense de época medioimperial (siglos II-III): la Dressel 2–4 evolucionada. SFECAG, Actes du Congrès de L'Escala-Empúries, pp. 281–286.
Járrega, R., Prevosti, M., 2011. *Figlinae tarraconenses*. La producció ceràmica a l'*ager Tarraconensis*. In: Prevosti, M., Guitart, i, Duran, J. (Eds.), Ager Tarraconensis 2. El poblament/The Population, Documenta 16. Institut d'Arqueologia Clàssica, Tarragona, pp. 455–490.
Kirschvink, J.L., 1980. The least-squares line and plane and the analysis of paleomagnetic data. Geophys. J. R. Astron. Soc. 62, 699–718.
Korte, M., Donadini, F., Constable, C.G., 2009. Geomagnetic field for 0–3 ka: 2. A new series of time-varying global models. Geochem. Geophys. Geosyst. 10, Q06008.
Korte, M., Constable, C., 2011. Improving geomagnetic field reconstructions for 0–3 ka. Phys. Earth Planet. Inter. 188, 247–259.
Kovacheva, M., Boyadziev, Y., Kostadinova-Avramova, M., Jordanova, N., Donadini, F., 2009. Updated archaeomagnetic data set of the past 8 millennia from the Sofia laboratory, Bulgaria. Geochem. Geophys. Geosyst. 10, Q05002.
Le Ny, F., 1988. Les fours de tuiliers gallo-romains, Éditions de la Maison des sciences de l'homme, Documents d'archéologie française, Paris.
Leonhardt, R., 2006. Analyzing rock magnetic measurements: the RockMagAnalyzer 1.0 software. Comput. Geosci. 32, 1420–1431.
López Mullor, A., Martín, A., 2008. Tipologia i datació de les àmfores tarraconenses produïdes a Catalunya. In: López Mullor, A., Aquilué, X. (Eds.), La producció i el comerç de les àmfores de la Província Hispania Tarraconensis. Homenatge a Ricard Pascual i Guasch, Monografies del Museu d'Arqueologia de Catalunya, vol. 8, pp. 33–94. Barcelona.
Moskowitz, B.M., 1980. Theoretical grain-size limits for single-domain, pseudo-single-domain and multi-domain behavior in titanomagnetite (X = 0.6) as a function of low-temperature oxidation. Earth Planet. Sci. Lett. 47, 285–293.
Nolla, J.M., Prados, A., Rojas, A., Santamaria, P., Soler, A., 2004. La Terrisseria Romana del Collet de Sant Antoni de Calonge, La Bisbal d'Empordà. In: Martín, A., Mataró, M., Nolla, J.M. (Eds.), Setenes Jornades d'Arqueologia de les Comarques Gironines (La Bisbal d'Empordà, 4–5 june 2004), pp. 193–200.
Otiña, P., 2009. Memòria. Excavació arqueològica. Vil·la romana de Barenys. Salou (Tarragonès). Némesis SCCL, unpublished report. Arxiu del Servei d'Arqueologia del Departament de Cultura de la Generalitat de Catalunya.
Pavón-Carrasco, F.J., Rodríguez-González, J., Osete, M.L., Torta, M., 2011. A Matlab tool for archaeomagnetic dating. J. Archaeol. Sci. 38, 408–419.
Pavón-Carrasco, F.J., Osete, M.L., Torta, M., Gaya-Piqué, L.R., 2009. A regional archaeomagnetic model for Europe for the last 3000 years, SCHA.DIF.3K: applications to archaeomagnetic dating. Geochem. Geophys. Geosyst. 10, Q03013.
Prevosti, M., Abela, J., 2011. Prospeccions superficials sistemàtiques, intensives. Tarragona. In: Prevosti, M., Guitart, J. (Eds.), Ager Tarraconenis 3. El poblament/the population, Documenta 16, pp. 37–111.
Prevosti, M., Casas, Ll, Roig Pérez, J.F., Fouzai, B., Álvarez, A., Pitarch, À., 2013. Archaeological and archaeomagnetic dating at a site from the ager Tarraconensis (Tarragona, Spain): El Vila-sec Roman pottery. J. Archaeol. Sci. 40, 2686–2701.
Ruiz-Martínez, V.C., Pavón-Carrasco, F.J., Catanzariti, G., 2008. First archaeomagnetic data from northern Iberia. Phys. Chem. Earth, Parts A/B/C 33, 566–577.
Sanz, M., 1975. Hallazgos romanos en Reus. Bol. Arqueol., época IV, fasc. 129–132, 112–115.
Schnepp, E., Lanos, P., 2005. Archaeomagnetic secular variation in Germany during the past 2500 years. Geophys. J. Int. 163, 479–490.
Tauxe, L., Mullender, T.A.T., Pick, T., 1996. Potbellies, wasp-waists, and superparamagnetism in magnetic hysteresis. J. Geophys. Res. Solid Earth 101, 571–583.
Tema, E., Kondopoulou, D., 2011. Secular variation of the Earth's magnetic field in the Balkan region during the last eight millennia based on archaeomagnetic data. Geophys. J. Int. 186, 603–614.
Wolfman, D., 1991. Retrospect and prospect. In: Eighmy, J.L., Sternberg, R.S. (Eds.), Archaeomagnetic Dating. University of Arizona Press, Tucson, pp. 313–364.
Zananiri, I., Batt, C.M., Lanos, P., Tarling, D.H., Linford, P., 2007. Archaeomagnetic secular variation in the UK during the past 4000 years and its application to archaeomagnetic dating. Phys. Earth Planet. Inter. 160, 97–107.